

# Application of Theory of Hybrid Systems to Control the Switching of Buck Converter

Mohammed Benmiloud<sup>1</sup>, Atallah Benalia<sup>2</sup>, Taous Meriem LALEG KIRATI<sup>3</sup>

<sup>1,2</sup>LACoSERE Laboratory, Electrical Engineering Department, Amar Telidji University of Laghouat, Algeria

<sup>3</sup>Mathematical and Computer Sciences & Engineering Division, Building 1, 4103, KAUST, Kingdom of Saudi Arabia

<sup>1</sup>M.Benmiloud.lagh@gmail.com; <sup>2</sup>a.benalia@mail.lagh-univ.dz

<sup>3</sup>taousmeriem.laleg@kaust.edu.sa

**Abstract-** The field of power electronics poses challenging control problems that can't be treated in a complete manner using traditional modeling. In this paper, the buck converter operating in Continuous Conduction Mode (CCM) is represented analytically by hybrid automaton model and graphically representation is also given. The hybrid trajectory and the model behavior are presented. The control problem of buck switching converters is transformed to a guard selection problem. The guard selection calculation formulas of buck converter are derived from the basic circuit laws. The stability of the switching is established analytically by the use of multiple Lyapunov functions to ensure the convergence and Poincare map to assess the local stability of the limit cycle. Numerical results clearly bring out the advantages and effectiveness of the proposed control law under varying line voltage and load conditions. Simulation studies are carried out in Matlab/Simulink/Stateflow.

**Keywords-** Buck Converter; Hybrid Modeling; Hybrid Trajectory; Multiple Lyapunov functions; Stabilization

## I. INTRODUCTION

Power converters are widespread industrial devices used, for example, in variable speed motor drives, computer power supply, cell phones and cameras and so on. Switch mode dc to dc converters are used to transform the unregulated dc input into a controlled dc output at a desired voltage level, in spite of line voltage, load current and temperature variations. This transformation is achieved by the use of semiconductor devices that operate as power switchers, turning on and off with high switching frequency.

The presence of switching makes the understanding of switched-mode converters not straightforward. Hence, converter modelling is central to the study of power electronics. To capture the evolution of these systems, mathematical models are needed that combine the dynamics of the continuous parts of the system with the dynamics of the discrete parts. Such hybrid systems contain both continuous and discrete states that influence the dynamic behaviour. There has been an increasing interest in these types of systems during the last decade, mostly due to the growing use of computers in the control of physical plants but also as a result of the hybrid nature of physical processes.

Traditionally, power electronics circuits and systems have been controlled in industry using linear controllers combined with nonlinear procedures like pulse width modulation (PWM). The models used for controller design are a result of simplifications that include averaging the

behaviour of the system over time (to avoid modelling the switching) and linearized around a specific operating point. As a result, the derived controller usually performs well only in neighbourhood around the operating point. Therefore, a novel method is desired for dc-dc converters by considering switching property explicitly as hybrid dynamical systems<sup>[1][2][3]</sup>.

The method in this paper, however, requires no averaging. The buck converter operating in CCM is represented analytically by hybrid automaton with graphically representation. The model behaviour and the hybrid trajectory are represented to provide insight the evolution of the hybrid dynamical system. The control problem of buck switching converter is given by the guard selection based on the mathematical representation of a trajectory which is approximated with respect to a real trajectory. The stability of the switching under this control scheme is established analytically by the use of multiple Lyapunov functions and Poincare approach<sup>[4][5]</sup>.

## II. HYBRID MODELLING OF THE BUCK CONVERTER

The topology of a DC-DC buck converter shown in the Fig. 1, contains a resistor load  $R$ , a filter capacitor  $C$ , an inductor  $L$  with role of energy storing, and two complementary switches: a power MOSFET used as a controlled power device  $SW$  and an uncontrolled device (diode  $D$ ). The output voltage  $v_o(t)$  of the buck converter is always lower than the input voltage  $E$ .

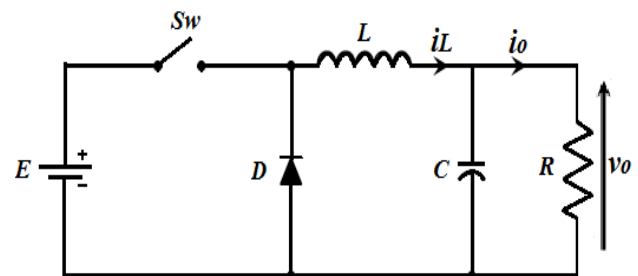


Fig. 1 Topology of buck converter

The buck converter can operate in a continuous conduction mode (CCM) or in a discontinuous conduction mode (DCM), depending on the waveform of the inductor current. In CCM the inductor current flows during the entire cycle, whereas in DCM the inductor current flows only during part of the cycle. In DCM it falls to zero, remains at

zero for some time interval, and then starts to increase. Operation at the CCM/DCM boundary is called the critical mode [1]-[6].

In the case of CCM, each mode of operation (given by the discrete state  $q$ ), the evolution of the continuous state variables  $x$  can be described by a different differential equations. Thus, the buck converter can be considered to be a hybrid dynamical system HDS where there is no jump in its state variables during the discrete transition.

A. Hybrid Automaton of DC-DC Buck Converter

Although many different models have been proposed in literature, the model ingredients are basically the same [1]. The hybrid model of the buck converter is completely described by the following system [7][8]:

$$H = (Q, \Sigma, X, Y, Init, S_c, S, T, Inv, Guard, Reset)$$

Where:

- $Q = \{q_i, i \in \{1, 2\}\}$  two discrete states representing Mode 1 and Mode 2 depending on the switch position (SW) and conducting of the diode (D);
- $\Sigma = \{\sigma_1, \sigma_2\}$  two controllable discrete inputs;
- $X = IR^+ \times IR^+, Y = IR^+$  are, respectively, the continuous state space and the continuous output space. The buck converter has two continuous states, the inductor current  $x_1 = i_L$  and the output voltage  $x_2 = v_o$ . The output considered here is the inductor current;
- $Init \in X \times Q$  is the set of initial states;
- $S_c$  is a subclass of dynamic systems.  $S_i \in S_c = \{S_1, S_2\}$  is defined by the equation in continuous time as :

$$\dot{x}(t) = f_{q_i}(x(t)), q_i \in Q$$

**Mode 1 ( $q=q_1$ ):**  $Sw$  is closed, the diode is on inverse polarization and can be eliminated for analysis. The dynamic of the resulting electrical system (Fig. 2) is given by,

$$\dot{x} = A_{q_1}x + B_{q_1}, A_{q_1} = \begin{bmatrix} 0 & -1 \\ 1 & -1 \\ C & RC \end{bmatrix}, B_{q_1} = \begin{bmatrix} E \\ L \\ 0 \end{bmatrix}$$

Where  $x = \begin{bmatrix} i_L \\ v_o \end{bmatrix}$  is the continuous state vector.

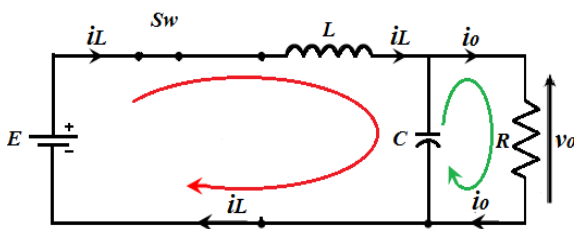


Fig. 2 Buck converter in Mode 1

The inductor current  $i_L$  flows through the switch. During this time interval, the energy is transferred from the dc input voltage source  $E$  to the inductor, capacitor, and load [6].

**Mode 2 ( $q=q_2$ ):**  $Sw$  is open, the inductor current continues to flow in the same direction after the switch turns off. Therefore, the inductor L acts as a current source, which forces the diode to turn on (directly polarized). The resulting circuit (Fig. 3) is described by the dynamic equations:

$$\dot{x} = A_{q_2}x + B_{q_2}, A_{q_2} = \begin{bmatrix} 0 & -1 \\ 1 & -1 \\ C & RC \end{bmatrix}, B_{q_2} = \begin{bmatrix} 0 \\ 0 \end{bmatrix}$$

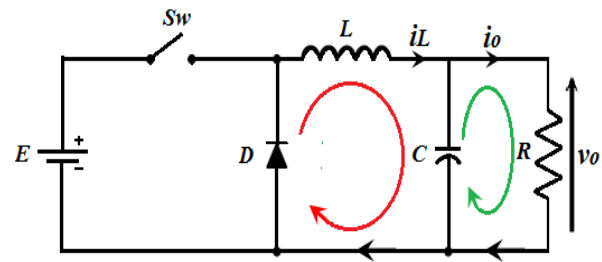


Fig. 3 Buck converter in Mode 2

The inductor L and capacitor C form an energy sources that maintains the load voltage and current when the switch is OFF.

Finally, we have:

$$f_{q_i}(x(t)) = \begin{cases} f_{q_1}(x(t)) = A_{q_1}x + B_{q_1} & \text{if } q(t) = q_1 \\ f_{q_2}(x(t)) = A_{q_2}x + B_{q_2} & \text{if } q(t) = q_2 \end{cases}$$

- $S$  is an application that associates to each discrete state  $q \in Q$  a continuous dynamic  $S_i \in S_c$ ;
- $T = \{T_{12} = (q_1, \sigma_1, q_2), T_{21} = (q_2, \sigma_2, q_1)\} \in Q \times \Sigma \times Q$  the transition relation;
- $Inv: Q \rightarrow 2^X$ , the invariants of modes. Where  $2^X$  denotes the power set of X, i.e., the collection of subsets of X. Each mode has an invariant associated to it, which describes the conditions that the continuous state has to satisfy at this mode. In open loop, we have  $Inv(q_1) = Inv(q_2) = IR^+ \times IR^+$ .
- $Guard: T \rightarrow 2^X$  is the guard condition; it describes a region in the state space X, if the state x is in this region, a discrete state transition may occur; we have  $Guard(T_{12}) = Guard(T_{21}) = IR^+ \times IR^+$  in open loop;

Invariants and guards play complementary roles: Whereas invariants describe when a transition must take place, namely when otherwise the motion of the continuous state would lead to violation of the conditions given by the invariant, the guards serve as “enabling conditions” that describes when a particular transition may take place [1].

- $Reset: T \times X \rightarrow IR^2$  is the reset map, it specifies how new continuous states are related to previous continuous states for a particular transition. For the

buck converter:  $Reset(., x(t^-)) = x(t^+)$ , it presents no jumps in the continuous state variables.

The hybrid state of the system H is given by  $(q, x) \in Q \times X$ .

Whereas the discrete state  $q$  influences the continuous dynamics by selecting a specific vector field  $f_{q_i}(x(t))$ , the influence of the continuous dynamics on the discrete state evolution is represented by a set of guards and invariants.

The elements of the hybrid automaton model lead to a graphical representation of the hybrid system (Fig. 4). Each node of the directed graph represents a mode (operating point) given by a system of differential equations. The arrows indicate the possible discrete transitions that correspond to a change of the mode.

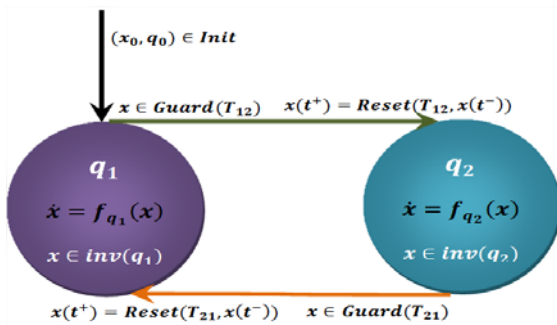


Fig. 4 Schematic representation of a hybrid automaton with two discrete states of the Buck converter operating in CCM

**B. Hybrid Trajectory**

The trajectories of the hybrid systems are partitioned into several time intervals. Within all intervals the continuous signals change smoothly and the discrete state remains constant [9].

The hybrid trajectory  $(I, q, x, y), I = \{I_k\}, k = 1, \dots, N$  is the

hybrid time and  $\begin{cases} q: I \rightarrow Q \\ x: I \rightarrow X \\ y: I \rightarrow Y \end{cases}$  is given by,

$$\begin{cases} \forall t \in I_k, q(t) = q_i, i = \{1, 2\}, k = \{1, 2, \dots, N\} \\ \forall t \in I_k, x(t) = \begin{cases} x(t_k^+) + \int_{t_k}^t f_{q_1}(x(t))dt & \text{if } i = 1 \\ x(t_k^+) + \int_{t_k}^t f_{q_2}(x(t))dt & \text{if } i = 2 \end{cases} \\ x(t_k^+) = \begin{bmatrix} i_L(t_k^+) \\ v_o(t_k^+) \end{bmatrix} = \text{Reset}(T_{ij}, x(t_k^-)) \\ \text{where } x(t_k^-) \in \text{Guard}(T_{ij}), (i, j = \{1, 2\}, i \neq j) \end{cases}$$

$t_k$  denotes any time instant at which at state is on the switching set.

$x(t_k^-)$  and  $x(t_k^+)$  denote the (limit) values of  $x(t)$  just before and just after the state jump, respectively. In this case,  $x(t_k^+) = x(t_k^-)$  presents no jumps.

**III. CONTROL SCHEME**

In steady state, the desired hybrid trajectory of inductor current and output voltage of a CCM operated buck converter can be approximated as shown in Fig. 5.

The current through the inductor  $i_L$  satisfies the following equations:

$$\begin{cases} i_L(t) = \frac{E - V_o}{L}t + I_{\min} & t \in [0, DT] \\ i_L(t) = \frac{-V_o}{L}(t - DT) + I_{\max} & t \in [0, DT] \end{cases}, \quad (1)$$

For a buck converter, the voltage ratio is given by,

$$D = \frac{V_o}{E}, \quad (2)$$

The change in inductor current  $\Delta i_L = I_{\max} - I_{\min}$ , in the interval  $[0; DT]$ , is given by,

$$\Delta i_L = \frac{(E - V_o)}{L}DT, \quad (3)$$

The electric charge stored in the capacitor during a switching period, is equal with the shade area from the Fig. 5, is given by [10],

$$Q = 2\Delta v_o C = \frac{1}{2}(I_{\max} - I_o)(t_1 + t_2),$$

Where  $V_o, I_o = \frac{V_o}{R}$  are the average output voltage and the average inductor current respectively (Fig. 5). Application of Thales' theorem, give us,

$$\frac{t_1}{DT} = \frac{t_2}{(1-D)T} = \frac{t_1 + t_2}{T} = \frac{I_{\max} - I_o}{I_{\max} - I_{\min}}$$

Thus, the change in charge stored during this period is related to the voltage ripple as:

$$\Delta v_o = \frac{\Delta i_L T}{16C}, \quad (4)$$

Using (2) in (3) to get an expression for  $T$  and using it in (4), we obtain,

$$\Delta v_o = \frac{\Delta i_L^2 LE}{16V_o(E - V_o)C}, \quad (5)$$

Equation (5) gives a relation between the ripple in inductor current to the ripple in output voltage for a buck converter operating in CCM. To generate the desired hybrid trajectory, we use (5) to define guard conditions and invariant of locations given by [4],

$$\begin{cases} \text{Inv}(q_1) = \left\{ x \in \mathbb{R}^2 / i_L \leq I_o + \frac{\Delta i_L}{2}, v_o \leq E \right\} \\ \text{Inv}(q_2) = \left\{ x \in \mathbb{R}^2 / i_L \geq I_o - \frac{\Delta i_L}{2}, v_o \leq E \right\} \\ \text{Guard}(T_{12}) = \left\{ x \in \mathbb{R}^2 / i_L = I_o + \frac{\Delta i_L}{2} \right\} \\ \text{Guard}(T_{21}) = \left\{ x \in \mathbb{R}^2 / i_L = I_o - \frac{\Delta i_L}{2} \right\} \end{cases}, \quad (7)$$

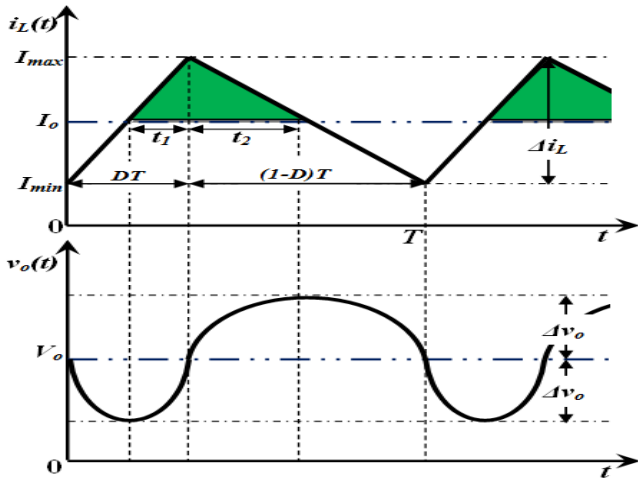


Fig. 5 The waveforms of inductor current and output voltage in steady state

By following these guards, the system will reach a limit cycle of constant frequency and constant amplitudes (Fig. 6) for an operating condition in CCM.

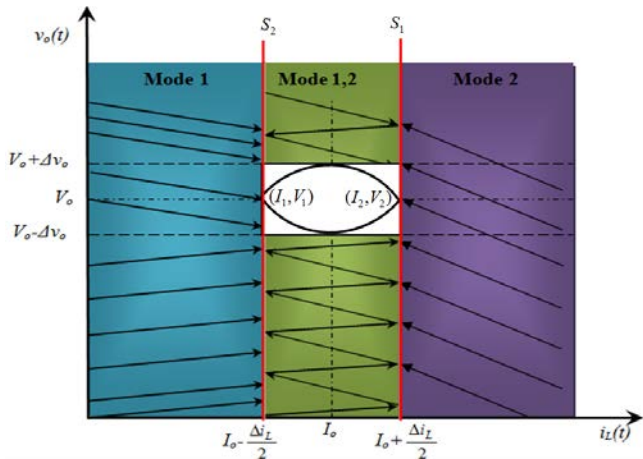


Fig. 6 Phase plane presenting the convergence of the buck converter

To provide insight in the evolution of the hybrid dynamical system under this control scheme, we give a short, rather informal description.

The initial hybrid state  $(q(0), x(0)) = (q_1, x_0)$ , Switch turns on, of trajectories of a hybrid automaton lies in the initial set *Init*. From this hybrid state the continuous state  $x$  evolves according to the differential equation:

$$\dot{x} = f_{q_1}(x) \text{ with } x(0) = x_0 \in \prod_x(\text{Init})$$

The discrete state  $q$  remains constant:  $q(t) = q_1$ . The continuous evolution can go on as long as the inductor current doesn't hit the switching surface given by the *Guard*( $T_{12}$ ). If at the instant  $t_k$  the continuous state reaches the *Guard*( $T_{12}$ ), we say that the transition  $(q_1, q_2)$  is enabled. The discrete state changes to  $q_2$  without continuous state jump because the inductor current and the output voltage waveform is a continuous function of time. After this transition, the continuous evolution resumes according to the mode  $q_2$  and the whole process is repeated [1]. The "hybrid phase portrait" is given by Fig. 7.

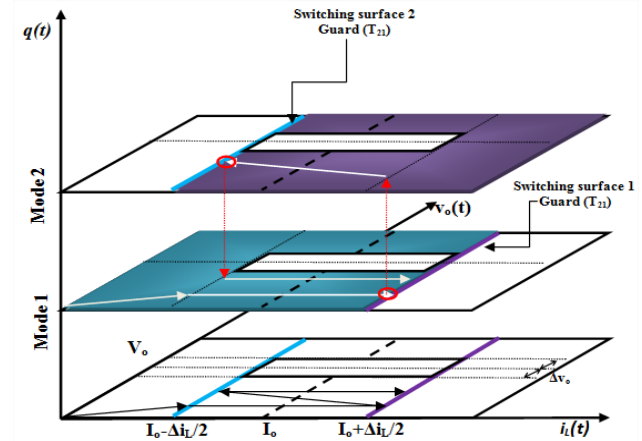


Fig. 7 Evolution of the hybrid state  $(q, x)$  of the buck converter after selection of the guard conditions

#### IV. STABILITY ANALYSIS

It is observed from Fig. 6 that under that proposed control scheme the system trajectory reaches a limit cycle. The local stability of the limit cycle can be proved by the Poincare map and to ensure the convergence we will use the multiple Lyapunov functions.

##### A. Convergence to the Steady Zone

This method requires different Lyapunov functions in all modes. All these Lyapunov functions should be positive and decreasing in the corresponding mode. Switching between the modes is governed by an additional condition, which ensures the stability of this switching [11].

For the given DC-DC buck converter circuit we define the following Lyapunov functions for each mode.

**Model1:** The Lyapunov function for this mode is the energy function  $L_1$  that is given as:

$$L_1 = \frac{1}{2}L(I_{\max} - i_L + \varepsilon)^2 + \frac{1}{2}C(V_o + \Delta v_o - v_o + \varepsilon)^2$$

Since this is a square function so it will be positive,  $L_1 > 0$ . The derivative of this will be negative as shown below:

$$\frac{dL_1}{dt} = - \left[ (I_{\max} - i_L + \varepsilon)(E - v_o) + (V_o + \Delta v_o - v_o + \varepsilon) \left( i_L - \frac{v_o}{R} \right) \right]$$

We have in  $inv(q_1)$ :

$$\begin{cases} i_L < I_{\max} + \varepsilon \Rightarrow (I_{\max} - i_L + \varepsilon) > 0 \\ v_o < E \Rightarrow E - v_o > 0 \\ v_o < V_o + \Delta v_o + \varepsilon \Rightarrow (V_o + \Delta v_o - v_o + \varepsilon) > 0 \\ 0 \leq i_L < \frac{E}{R} + \Delta i_L \\ 0 \leq \frac{v_o}{R} < \frac{E}{R} \end{cases} \text{ leads to } 0 \leq (i_L - \frac{v_o}{R}) < \Delta i_L$$

Thus,

$$\frac{dL_1}{dt} < 0, \left[ \begin{matrix} i_L \\ v_o \end{matrix} \right] \in inv(q_1)$$

So this function is positive and decreasing during this mode. Thus  $L_1$  is a Lyapunov function for mode 1.

**Mode2:** The energy function  $L_2$  for this mode is given as:

$$L_2 = \frac{1}{2}L(I_{\min} - i_L - \varepsilon)^2 + \frac{1}{2}C(V_o + \Delta v_o - v_o + \varepsilon)^2$$

This function is positive,  $L_2 > 0$  and its derivative is given by,

$$\frac{dL_1}{dt} = - \left[ (I_{\min} - i_L - \varepsilon)(-v_o) + (V_o + \Delta v_o - v_o + \varepsilon) \left( i_L - \frac{v_o}{R} \right) \right]$$

We have in  $inv(q_2)$ :

$$\begin{cases} i_L > I_{\min} - \varepsilon \Rightarrow (I_{\min} - i_L - \varepsilon) < 0 \\ v_o > 0 \Rightarrow -v_o < 0 \\ v_o < V_o + \Delta v_o + \varepsilon \Rightarrow (V_o + \Delta v_o - v_o + \varepsilon) > 0 \\ \begin{cases} i_L \geq I_{\min} \\ \frac{v_o}{R} \geq 0 \end{cases} \text{ leads to } \left( i_L - \frac{v_o}{R} \right) \geq I_{\min} \end{cases}$$

Thus,

$$\frac{dL_2}{dt} < 0, \begin{bmatrix} i_L \\ v_o \end{bmatrix} \in inv(q_2)$$

So this energy function is positive and decreasing, hence  $L_2$  is a Lyapunov function for Mode 2.

The simulation results show that these Lyapunov functions are a non-increasing sequence at the consecutive times obtained when switching to the different vector fields. Hence it is concluded that this switching scheme is stable.

**B. Limit Cycle Stability**

The theorem used to prove the limit cycle stability is re-stated below.

Assume there exists a limit cycle  $\gamma$  with period  $t^*$ . Assume also the limit cycle is transversal to the switching surfaces  $S_1, \dots, S_k$  at  $x_1^*, \dots, x_k^*$ , respectively. Let  $x_0^* \in S_k$  be the initial state that generates the periodic motion. Consider the map  $T$  from some point in a small neighborhood of  $x_0^*$  in  $S_k$ , to the point when the trajectory returns to  $S_k$ . Local stability of a limit cycle can be checked by looking at the poles of the linear part  $T$ . The Jacobian of the map  $T$  is given by  $W = W_k W_{k-1} \dots W_2 W_1$  where

$$W_i = \begin{pmatrix} I - \frac{v_i C_i}{C_i v_i} \end{pmatrix} e^{A_i t_i^*} \tag{8}$$

With  $v_i = A_{q_i} x_i^* + B_{q_i}$ ,  $i = 1, \dots, k$ . The limit cycle  $\gamma$  is locally stable if  $W$  has all its eigenvalues inside the unit disk. It is unstable if at least one of the eigenvalues is outside the unit disk<sup>[12]</sup>.

As shown in Fig. 6, the CCM operation of buck converter has two modes of operation and hence two trajectories are part of the limit cycle in CCM. The switching surfaces in mode switched control are given

by  $C_i x + d_i$ , where  $C_1 = C_2 = [1 \ 0]$ ,  $d_1 = -(I_o + \Delta i_L / 2)$  and  $d_2 = -(I_o - \Delta i_L / 2)$ . Let the switch points on  $C_1$  and  $C_2$  are  $x_1^* = [I_1 \ V_1]^T$  and  $x_2^* = [I_2 \ V_2]^T$  respectively (Fig. 6). Based on (8) and substituting parameters by their values, we obtained the Jacobian of Poincare map in each mode.

$$W_1 = \begin{pmatrix} 0 & 0 \\ -\frac{L}{RC} \frac{(I_1 R - V_1)}{(E - V_1)} & 1 \end{pmatrix} e^{A_{q_1} t_1^*}$$

$$W_2 = \begin{pmatrix} 0 & 0 \\ \frac{L}{RC} \frac{(I_2 R - V_2)}{V_2} & 1 \end{pmatrix} e^{A_{q_2} t_2^*}$$

The switching instants can be obtained from (3) and (4).

$$\begin{cases} t_1^* = DT = \frac{L \Delta i_L}{E - V_o} \\ t_2^* = (1 - D)T = \frac{L \Delta i_L}{V_o} \end{cases}$$

The Jacobian of the Poincare map is given by,

$$W = W_2 W_1$$

The limit cycle is locally asymptotically stable if the eigenvalues of the above matrix are within the unit disk. It's clear that one eigenvalue of  $W$  is zero and is inside the unit circle and the second eigenvalue is given in fig .8 for different values of load resistance and output voltage reference. Fig. 8 shows that the second eigenvalue is always inside the unit circle under variable desired voltage and load resistance. Hence, the limit cycle formed under such conditions is always asymptotically stable. This confirms the stability of switching of the proposed hybrid control scheme. The parameters of the buck converter are given in the next section.

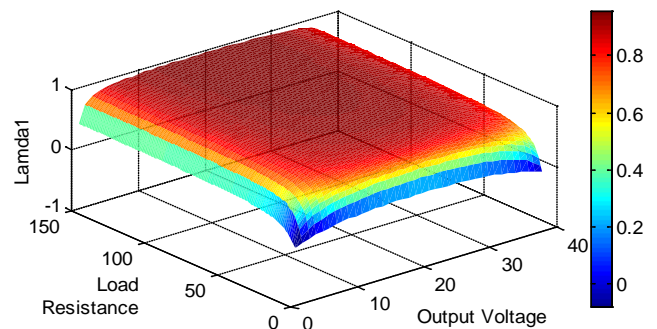


Fig. 8 Values of the eigenvalue of the Jacobian Poincare map for variable desired voltage and load resistance

**V. SIMULATION OF A TYPICAL BUCK CONVERTER UNDER THE PROPOSED SCHEME**

The values of the parameters of the buck converter used in simulations, using Matlab-Simulink-Stateflow<sup>[13]</sup>, are:

$$\begin{matrix} E=40V & R=20\Omega & C=10\mu F \\ L=0.35mH & V_o=20V & \Delta v_o=0.01V \end{matrix}$$

Fig. 9 presents the output voltage and inductor current evolutions for a variable reference voltage  $V_o$ . The obtained result shows that the control is able to drive the system quickly towards the set point without undergoing any overshoot in output voltage.

Fig. 10 shows the phase plane of the buck converter, it has limit cycle to which trajectories starting from other initial conditions appear to be attracted.

Fig. 11 is an enlarged version of Fig. 9 and the corresponding discrete state evolution.

Fig. 12 shows the robustness of the control law under the perturbation (varying of the load resistance), as we can see that the perturbation is rejected and the output voltage maintain the constant voltage where the load on the system (resistor) is increased at  $t=3ms$  by  $40\Omega$  and decreased at  $t=6ms$  by  $50\Omega$  and increased at  $t=9ms$  by  $20\Omega$ .

Fig. 13 shows in other hand the effectiveness of the proposed control under the variation of the input voltage where the input voltage  $E$  is increased at  $t=3ms$  by  $10V$  and decreased by  $15V$  at  $t=6ms$  then it is increased by  $5V$  at  $t=9ms$ .

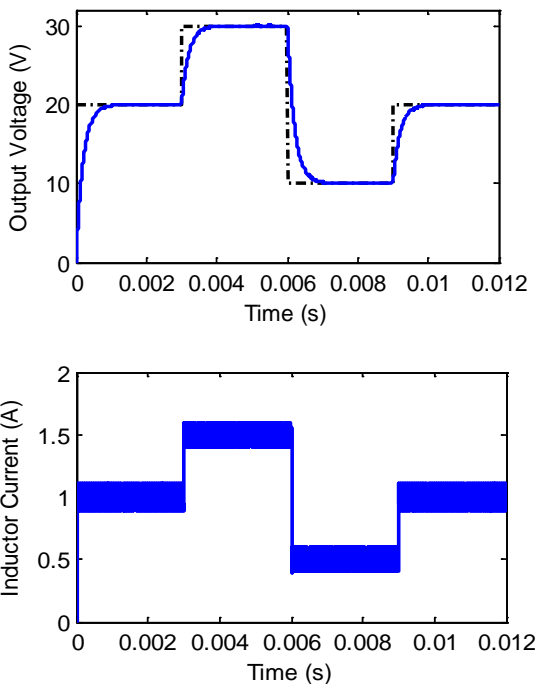


Fig. 9 Output voltage and inductor current evolutions for variable desired voltage

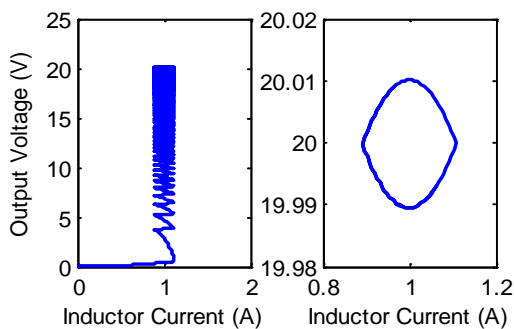


Fig. 10a) Phase plane of the buck converter .b) Steady behavior presents limit cycle.

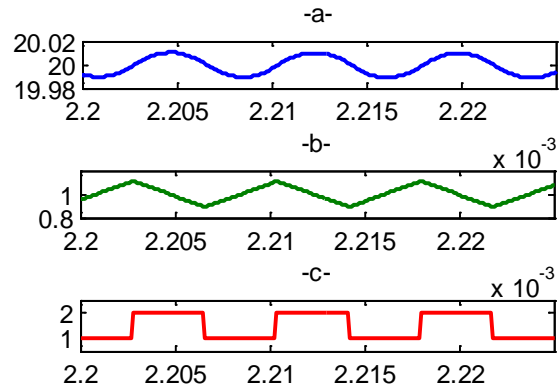


Fig. 11 Stationary behavior of the buck converter a) Output Voltage b) Inductor current c) Discrete state

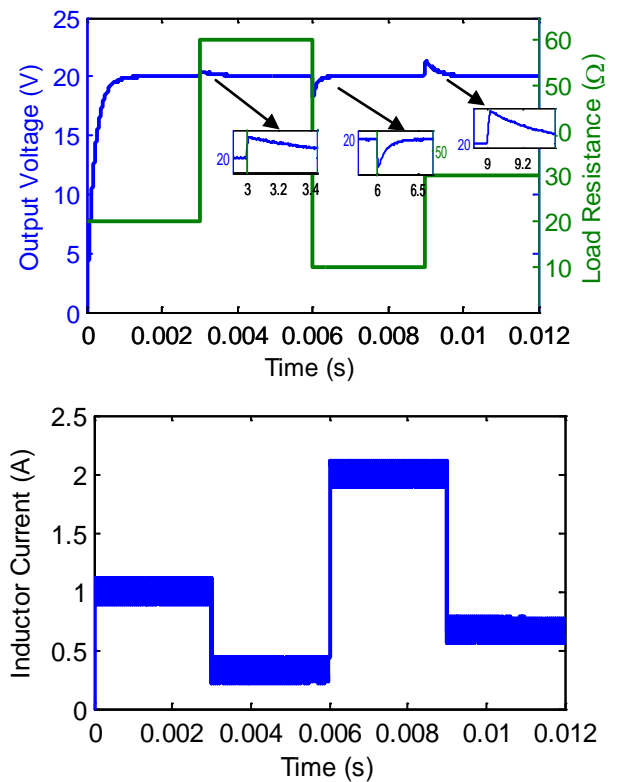


Fig. 12 Output voltage and inductor current evolutions with the variation of the load resistance

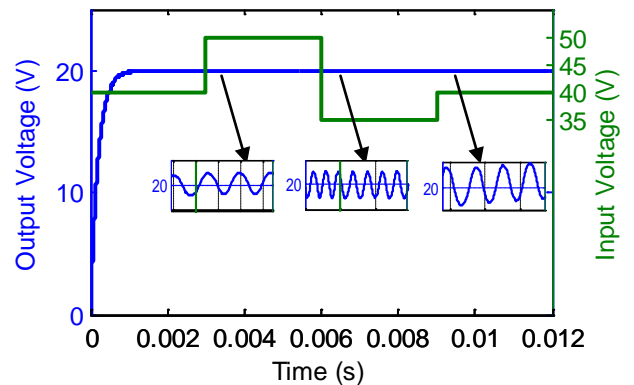


Fig. 14 shows the evolution of the Lyapunov functions where the decrease of energy is illustrated in each mode and also in the consecutive times obtained when switching to the different vector fields.

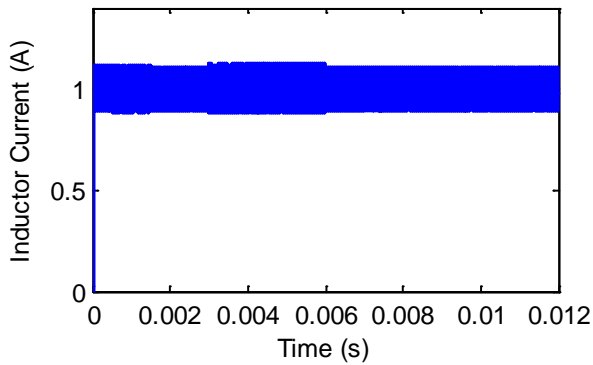


Fig. 13 Output voltage and inductor current evolutions with the variation of the input voltage

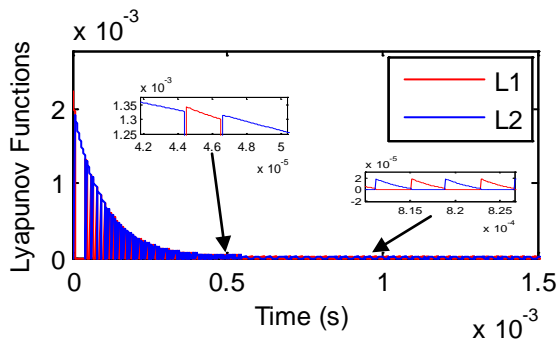


Fig. 14 Evolution of the Lyapunov functions

## VI. CONCLUSIONS

Hybrid modeling and guard selection for the model and control of the buck converter are proposed in this paper. It is also shown that this scheme is stable by using the theory of multiple Lyapunov functions and Poincare approach. The simulation results confirm the advantage of this control scheme and specially its performance and robustness under various perturbations.

## REFERENCES

- [1] J. Lunze., Handbook of hybrid systems control, Theory, Tools, Applications. Cambridge University press: United States of America, pp. 3–30, 2009.
- [2] S. Sanders, J.M. Noworolski, X.Z. Liu, G.C.V. Sender, and J.M. Noworolski, “Generalized averaging method for power conversion circuits,” *IEEE Transactions on Power Electronics*, vol. 6, pp.251-159, April, 1991.
- [3] T. Geyer, G. Papafotiou, and M. Morari, “Model Predictive Control in Power Electronics: A hybrid Systems Approach,” *Proceedings of the 44<sup>th</sup> IEEE Conference on Decision and Control, and the European Control Conference 2005*, pp. 5606–5611, December, 2005.
- [4] C. Sreekumar, V. Agarwal, “A simple hybrid mode switching control law for a buck converter and its stability analysis,” *Proceedings of the International Conference on Advances in Control and Optimization of Dynamical Systems ACODS*, pp. 384 –389, 2007.
- [5] P. Gupta, A. Patra, “A stable Energy-Based Control Strategy for DC-DC Boost Converter Circuits,” *35<sup>th</sup> Annual IEEE Power Electronics Specialists Conference*, Vol.5, pp. 3642 – 3646, June, 2004.
- [6] M.K. Kazimierczuk, Pulse-width Modulated DC–DC Power Converters .AJohn Wiley and Sons, Ltd, Publication: United Kingdom, 2008.
- [7] A. Birouche, “Contribution sur la synthèse d’observateurs pour les systèmes dynamiques hybrides,” Ph.D. Thesis, Lorraine Graduate School, Vandœuvre-lès-Nancy Cedex, France, 2006.
- [8] E. Zulueta, T. Rico, J.M.G. Durana, “Hybrid Modeling Of Open Loop DC-DC Converters”, *Revista Facultad De Ingenieria U.T.A(Chile)*, Vol. 11, No. 2, pp. 41-47, 2003.
- [9] A. Girard, “Analyse Algorithmique des Systèmes Hybrides,” Ph.D. Thesis, National Polytechnic School of Grenoble, France, 2004.
- [10] E.P. Leite, Matlab-Modelling, Programming and simulations, Janeza Trdine 9, 51000 Rijeka, Croatia, 2010.
- [11] S. Pettersson, “Analysis and Design of Hybrid Systems,” Ph.D. Thesis, Chalmers University of Technology, Göteborg, Sweden, 1999.
- [12] J.M.M.S. Gonçalves, “Constructive Global Analysis of Hybrid Systems,” Ph.D. Thesis, Massachusetts Institute of Technology, USA, 2000.
- [13] S.T. Karris., Introduction to State flow with Applications, Orchard Publications, 2007.